Bioinorganic Chemistry

DOI: 10.1002/ange.201304021

Single Glutamate to Aspartate Mutation Makes Ferric Uptake Regulator (Fur) as Sensitive to H_2O_2 as Peroxide Resistance Regulator (PerR)**

Aubérie Parent, Christelle Caux-Thang, Luca Signor, Martin Clémancey, Ramakrishnan Sethu, Geneviève Blondin, Pascale Maldivi, Victor Duarte, and Jean-Marc Latour**

One major recent advance in the field of metals in biology was the discovery that metal homeostasis is tightly controlled by sophisticated protein machineries that import metals, regulate their concentration, and distribute it among target proteins.[1] These machineries are under the control of specific transcription factors that are able to detect their cognate metal. These metalloregulators have recently been classified according to their structural properties into several families, one of which is the Fur family that is present in many Gram-negative and Gram-positive bacteria.[2] It comprises four proteins involved in metal homeostasis Fur (ferric uptake regulator), Mur, Nur, and Zur that regulate Fe, Mn, Ni, and Zn concentration, respectively. The last member of the family, PerR, is not involved in metal homeostasis but is a peroxide resistance regulator, functionally equivalent to OxyR.[3] Indeed, the PerR regulon comprises peroxide defense enzymes (KatA, AhpCF) and a DNA protection protein (MrgA), and it is induced by reaction of PerR with H_2O_2 that leads to PerR oxygenation.[4,5] All the biochemical and structural evidence indicates a strong similarity between Fur and PerR, albeit Fur does not react with H_2O_2. Herein, we aimed to understand the molecular basis of these distinct behaviors. Both are dimeric proteins that possess the same overall fold and each monomer is able to bind two metal ions: Zn^{2+} in a structural binding site and in the regulatory site their cognate metal (Fe^{2+} for Fur and Fe^{2+} or Mn^{2+} for PerR). Figure 1 shows the sequence alignments of the structural and the regulatory binding sites for *Bacillus subtilis* PerR and for Fur proteins from *Bacillus subtilis* (*Bs*), *Helicobacter pylori* (*Hp*), and *Escherichia coli* (*Ec*).

```
                37 ------ 85
Bs PerR  VNSMAHPTAD SSRFDFVTSD
Bs Fur   ENEEDHLSAE DLRKDGAAHF
Hp Fur   YRSGTHLSPE -RRYEIAAKE
Ec Fur   EPDNHHVSAE -SVFELTQQH

 91   96 99   104   -----  136
-HYHAICENCG KIVDFHYPGL EIYGVCQECS
-HHHLVCMECG AVDEIEGDLL TFHGICHRCN
HHDHIICLHCG KIIEFADPEI KMFVWCKECQ
-HDHLICLDCG KVIEFSDDSI YLYGHCAEGD
```

Figure 1. Sequence alignments of selected PerR and Fur proteins highlighting the regulatory site (bold) and the structural site (italics). Numbering according to *Bs* PerR.

The crystal structure of *Bs* PerR-Zn-Mn shows that the coordination of the regulatory metal involves five residues arranged as a distorted square pyramid where H37, D85, H91, and D104 constitute the base of the pyramid and H93 occupies the apical position.[6] Binding of the H37 residue to the cognate metal is responsible for the structural change that allows the holoprotein to adopt the right conformation to bind DNA. In turn, oxidation of H37 or H91 by H_2O_2 abolishes the DNA-binding ability of PerR.

The sequence alignments presented in Figure 1 are very informative because they show that the only difference in the regulatory sites of PerR and Fur is the nature of the carboxylate ligands of the Fe^{2+} ion. On one hand, aspartate D104 in the PerR proteins is strictly changed to a glutamate (E) in all Fur proteins. On the other hand, aspartate D85 found in the majority of PerR proteins is changed to a glutamate in most Fur proteins, as for example in *Hp* Fur and *Ec* Fur but not in *Bs* Fur (Figure 1; see Supporting Information, Figure S1 for a more complete list). Because these changes in carboxylate ligands are the only ones apparent between PerR and Fur proteins, we hypothesized

[*] A. Parent, C. Caux-Thang, Dr. M. Clémancey, Dr. R. Sethu, Dr. G. Blondin, Dr. V. Duarte, Dr. J.-M. Latour
Univ. Grenoble Alpes, LCBM
38054 Grenoble (France)
and
CEA, DSV, iRTSV, LCBM, PMB
38054 Grenoble (France)
and
CNRS UMR 5249, LCBM
38054 Grenoble (France)
E-mail: victor.duarte@cea.fr
jean-marc.latour@cea.fr
Dr. L. Signor
Univ. Grenoble Alpes, IBS (France)
and
CNRS, IBS, Grenoble (France)
and
CEA, IBS, Grenoble (France)
Dr. P. Maldivi
Univ. Grenoble Alpes, UMR E 3 (France)
and
CEA, DSM, INAC, SCIB, RICC, Grenoble (France)

[**] J.-M.L. acknowledges the support of the Région Rhône-Alpes (contract CIBLE 07 016335), IFCPAR (Project No. IFC/4109-1), and Labex ARCANE (ANR-11-LABX-0003-01).

Supporting information for this article is available on the WWW under http://dx.doi.org/10.1002/anie.201304021.

that they are responsible for the differences in H_2O_2 reactivity. To investigate the potential role of these aspartate/glutamate residues, we mutated them in the *Bs* PerR and *Bs* Fur proteins and assessed their reactivity with H_2O_2 both in vivo and in vitro. Our results indicate that the H_2O_2 sensitivity of *Bs* PerR is strictly associated with D104 and is abolished by a D104E mutation, a result that is supported by the reverse E108D mutation making *Bs* Fur sensitive to H_2O_2. By combining Mössbauer spectroscopic studies and DFT calculations, we are able to propose a structural change to the Fe coordination sphere associated with D to E mutations.

To investigate the various possible combinations of carboxylate residues in the PerR and Fur regulatory sites, we prepared two single mutants and a double mutant of *Bs* PerR, namely D85E, D104E and D85E D104E, and the *Bs* Fur "reverse mutants" D85E and E108D to probe the influence of these mutations. In terms of Fe ligation, the *Bs* PerR-D104E mutant is equivalent to *Bs* Fur and the *Bs* PerR-D85E-D104E double mutant and *Bs* Fur-D85E mutant are equivalent to *Hp* and *Ec* Fur. All wild-type proteins and mutants were overexpressed under two different conditions: 1) LB medium that is known to produce an oxidized PerR-WT protein owing to reaction with endogeneously generated H_2O_2 and 2) minimal medium supplemented with an Fe scavenger, desferrioxamine, that produces non-oxidized PerR-WT protein. In both cases, the variants are isolated in dimeric form binding two Zn^{2+} ions but lacking the regulatory metal. We then used a global approach to assess the impact of the mutations on 1) the binding of the regulatory metal, taking into account that the affinity of PerR[7] and Fur[8] for Fe^{2+} is an order of magnitude higher than for Mn^{2+}, 2) the oxidation of the variant under both in vivo and in vitro conditions, and 3) the effect of oxidation on the His ligands of Fe, as in PerR.

The metal binding capacity of all variants was investigated by monitoring Mn^{2+} binding by EPR spectroscopy, as previously described.[5] All PerR and Fur mutants have Mn^{2+} affinities in the micromolar range, same as the WT proteins (Table S1). This indicates that the D/E or E/D mutations do not drastically affect the coordination ability of the protein[8] and that it is therefore likely that the PerR and Fur mutants bind to the Mn^{2+} ion in the regulatory site.

All variants overexpressed in LB medium and potentially oxidized were analyzed by ESI-MS to assess their sensitivity to endogeneously generated H_2O_2. Oxidation of PerR-WT was shown by a peak at m/z 16308 (16292 + 16) for the oxidized monomer (Figure 2), corresponding to the oxygenation of histidine H37 or H91.[4,5] Under these conditions, 63% of PerR-WT was oxidized and only 3% of PerR-D104E was oxidized. Similarly, the mutants PerR-D85E and PerR-D85E-D104E were oxidized to 64% and 0%, respectively

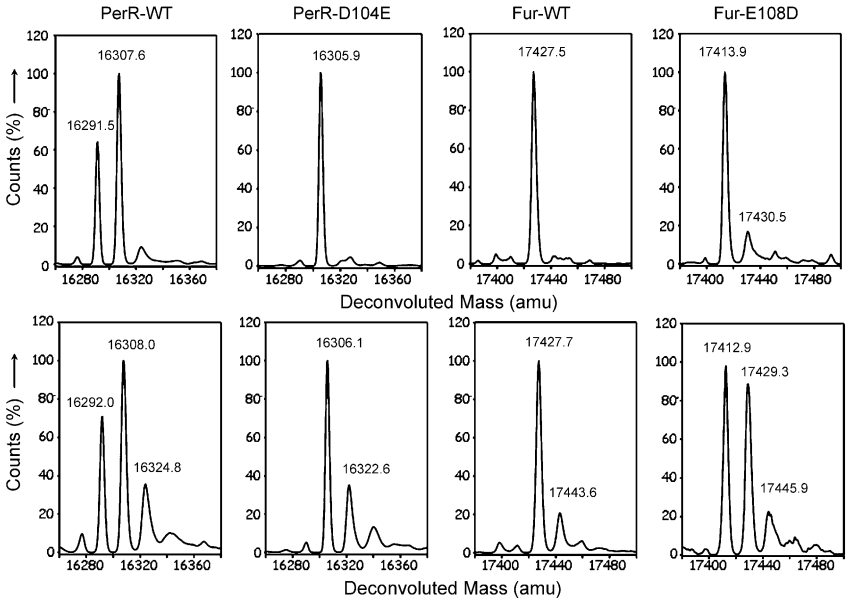

Figure 2. ESI-MS analysis of in vivo (top) and in vitro (bottom) oxidation of PerR-WT, PerR-D104E, Fur-WT, and Fur-E108D.

(Figure S2, Table S2). These results indicate that the sensitivity of PerR to oxidation is strictly controlled by the nature (Asp versus Glu) of the residue in position 104, whereas that in position 85 has no effect. The latter observation is consistent with the fact that both aspartate and glutamate can be found at position 85 in Fur proteins and that D85 in PerR is not strictly conserved, in contrast to D104. As shown in the top row of Figure 2, the same analysis revealed that Fur-WT and Fur-E108D mutant were oxidized to 4 and 14%, respectively, pointing to a slight increase in H_2O_2 sensitivity of the mutant. Because the endogenous oxidation during cell culturing could not be controlled, we complemented these in vivo experiments with in vitro oxidation of the isolated unoxidized variants (overexpressed in minimal medium), following metallation by one equivalent of Fe^{2+} ions and subsequent treatment with one equivalent of H_2O_2 under anaerobic conditions. The ESI-MS analyses (Figure 2, bottom row) revealed that PerR-WT was oxidized to a similar level (66%), while PerR-D104E was more oxidized (33%) than for the in vivo experiments but still significantly less than the wild type protein. Interestingly, Fur-WT was slightly oxidized (21%) but Fur-E108D was oxidized to a level (54%) comparable to PerR-WT. It is likely, that the lower concentration of H_2O_2 produced in vivo relative to the stoichiometric level of H_2O_2 used in vitro (50 μM) is responsible for the difference in sensitivity observed for these variants under the two conditions. These oxidation experiments clearly establish that the presence of an D104E mutation suppresses the oxidation sensitivity of PerR and that the reverse mutation (E108D) makes Fur sensitive to H_2O_2 oxidation (Table 1). By contrast, the D85E mutation seems to have no effect on the reaction of H_2O_2 with PerR and only a minor effect on Fur (See Figure S2 and Table S2 for oxidation of the PerR-D85E and Fur-D85E mutants).

Table 1: Oxidation and Mössbauer quadrupole splittings of *Bs* PerR and *Bs* Fur variants.

Bs PerR	oxidation[a] [%] in vivo	in vitro	ΔE_Q[b] [mm s^{-1}]	*Bs* Fur	oxidation[a] [%] in vivo	in vitro	ΔE_Q[b] [mm s^{-1}]
WT	63	66	3.05[c]	E108D	14	54	3.05[c]
D104E	3	33	3.25[c]	WT	4	21	3.21
D85E-D104E	0	23	3.46[c]	D85E	2	35	3.37

[a] See Figure S2 and Table S2 for the values of PerR-D85E-D104E and Fur-D85E. [b] Uncertainties are 0.04 mm s^{-1}. [c] These samples contained two components in ratios higher than 3 to 1. The values in the table are associated with the major component. Other values are in Table S4.

Electrophoretic mobility-shift assay (EMSA) experiments were performed, first to verify that the Fur-E108D mutant binds DNA in the presence of a regulatory metal and second to investigate whether in vitro oxidation of the mutant will affect its DNA binding capacity, which would show that this oxidation is directed to H37/H95, analogous to H37/H91 in PerR-WT. Figure 3 shows EMSA experiments performed with PerR-WT and Fur-E108D using DNA duplexes containing, respectively, the *per* box of the *mrgA* promoter and the *fur* box of the *feuA* promoter. The EMSA experiments done with Fur-WT and Fur-D85E are presented in Figure S3. Figure 3 shows the formation of the PerR-WT (a) and Fur-E108D (b) DNA complexes using increasing concentrations of both proteins in the presence of 100 μM Mn^{2+}. The K_d values estimated from these experiments are all in the nanomolar range (Table S3) in agreement with strong DNA binding. This shows that the mutation does not affect the DNA binding capacity of the mutant. Figure 3 c,d shows similar EMSA experiments but the proteins were treated with stoichiometric amounts of both Fe^{2+} ions and H_2O_2 prior to gel analyses. As expected for PerR-WT (c), these oxidative conditions largely affect the formation of the protein–DNA complex. Interestingly, the formation of the Fur-E108D-DNA complex (d) was almost abolished by this treatment. This observation suggests that oxidation of the Fur-E108D mutant occurs on the Fe binding histidines as in PerR. To verify it, after the H_2O_2/Fe^{2+} treatment, the Fur-E108D mutant was digested and the peptide fragments separated by HPLC and analyzed by ESI-MS. Figure 3 e,f illustrates the profiles of the two peptides P1 and P2 containing H37 and H95, respectively. These profiles show that the peroxide-induced oxidation occurs on the same peptides as in PerR-WT, thus supporting that it affects the two histidines that are Fe ligands.

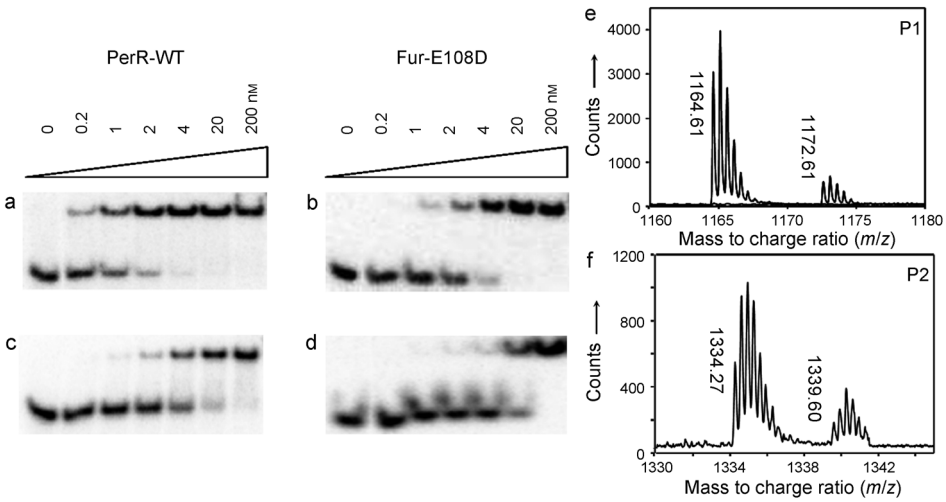

Figure 3. a–d) EMSA experiments of oxidation of PerR-WT (a,c) and Fur-E108D (b,d). a,b) protein incubated with Mn^{2+}; c,d) protein incubated with Mn^{2+} following H_2O_2/Fe^{2+} treatment and purification. e,f) LC–MS analyses of trypsin-digested Fur-E108D after H_2O_2/Fe^{2+} treatment. P1 = residues 29–48; P2 = residues 89–123. Overlay of MS spectra for both unoxidized $[P1+2H]^{2+}$ ions (retention time (RT) = 36.0 min) and oxidized $[P1+16+2H]^{2+}$ ions (RT = 37.3 min). MS spectra for both unoxidized $[P2+3H]^{3+}$ ions and oxidized $[P2+16+3H]^{3+}$. Oxidized and unoxidized P2 ions co-eluted with an RT of 49.2 min.

These observations point to a crucial role of the carboxylate 104 residue to control access of H_2O_2 to the Fe coordination sphere. Because carboxylates can adopt a variety of coordination modes to a metal ion, the observed protective effect of the D to E mutation is probably linked to a change in the carboxylate coordination mode that protects the Fe center from H_2O_2 attack. Unfortunately, there is no X-ray crystal structure available to date of a Fur protein with its regulatory metal Fe^{2+} ion or a structurally similar one (i.e. Mn^{2+}). The only reported structures have a Zn^{2+} ion in place of the regulatory metal[9–12] and with its d^{10} electronic structure Zn^{2+} is insensitive to ligand field and thus cannot reveal subtle changes in the coordination sphere of the regulatory metal. To understand this structural change at the molecular level we used a combination of Mössbauer spectroscopy and density functional theory (DFT) calculations, which have recently been used in concert to derive spectroscopically validated structural properties.[13–16] To get insights into the coordination changes brought about by the Asp/Glu substitutions, we decided to study PerR and Fur variants possessing the three carboxylate combinations Asp/Asp, Asp/Glu, and Glu/Glu in the 85 and 104 positions (with *Bs* PerR numbering). Figure 4 depicts the Mössbauer spectra of PerR-WT, PerR-D104E and PerR-D85E-D104E variants and Fur-WT, Fur-E108D, and Fur-D85E variants and the corresponding nuclear parameters are listed in Table 1 and Table S4. These parameters are consistent with ferrous centers in the high spin state $S = 2$. Whereas they appear very close, they reveal significant differences in the quadrupole splitting (QS) values. Indeed the two variants with two Asp PerR-WT and Fur-E108D have

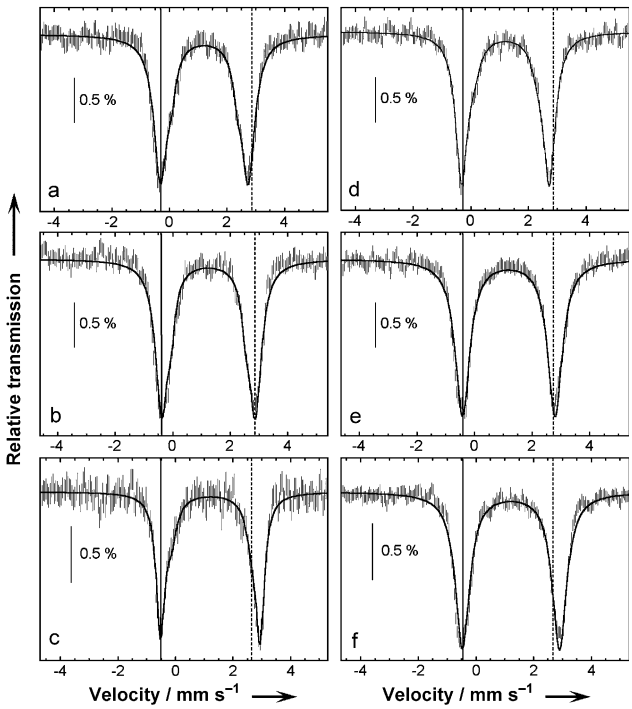

Figure 4. Mössbauer spectra of a) PerR-WT, b) PerR-D104E, c) PerR-D85E-D104E, d) Fur-E108D, e) Fur-WT, and f) Fur-D85E. Spectra are aligned according to the lower velocity absorption (solid vertical line). The dotted lines correspond to ΔE_Q values of 3.25 mm s^{-1} (left panels) and 3.21 mm s^{-1} (right panels).

the same value $\Delta E_Q = 3.05$ mm s^{-1}, whereas those having an Asp/Glu combination PerR-D104E and Fur-WT exhibit higher values $\Delta E_Q = 3.25$ mm s^{-1} and 3.21 mm s^{-1}, respectively. Those with two Glu residues PerR-D85E-D104E and Fur D85E exhibit even higher values $\Delta E_Q = 3.46$ mm s^{-1} and 3.37 mm s^{-1}, respectively, which are reminiscent of that determined earlier for *E. coli* Fur-WT $\Delta E_Q = 3.47$ mm s^{-1} that also possesses two Glu residues (Figure 1).[17] These differences of 0.20(3) mm s^{-1} appear small but they amount to approximately four times the uncertainty of the measurements and are thus reliable. These observations can be summarized as follows: the ferrous centers with two Asp residues have a QS close to 3.00 mm s^{-1}, those with an Asp/Glu combination have a QS close to 3.20 mm s^{-1}, and those with two Glu residues have a QS close to 3.40 mm s^{-1}. So each Asp to Glu substitution causes an approximately 0.20 mm s^{-1} increase in the QS of the Fe^{II} ion. These variations of the Mössbauer QS clearly indicate that the Asp to Glu mutations cause significant changes in the coordination sphere of the Fe center.

To get insights into the nature of these structural changes of the Fe centers and how they relate to the different H_2O_2 sensitivities, we developed a stepwise theoretical approach based on DFT structure calculations validated by calculation of the Mössbauer QS trend. We investigated three families of Fe^{2+} complexes as models for the three environments of iron with two Asp, one Asp/one Glu, and two Glu residues. First, to accurately calculate QS parameters that differ experimentally by 0.2 mm s^{-1}, we performed a detailed estimation of QS parameters for families of iron complexes chosen from Friesner and co-workers[13] to obtain a reliable basis for further estimations of these parameters on our models. Second, we chose starting structures based on the available experimental data. We extracted the Mn site from the PerR-Zn-Mn X-ray crystal structure,[6] keeping only the three His and two Asp residues directly involved in the square-pyramidal metal-coordination sphere. The adjustment in metal–ligand distances to account for the change from Mn^{2+} to Fe^{2+} was based on PerR-Zn-Fe EXAFS data.[6] The His residues were modeled by 4-methylimidazole following removal of the protein chain. Control calculations showed that modeling the carboxylate residues with acetates, thus removing the protein chain, introduced slight changes in QS. Thus, from this preliminary structure (Figure 5a), a two-step

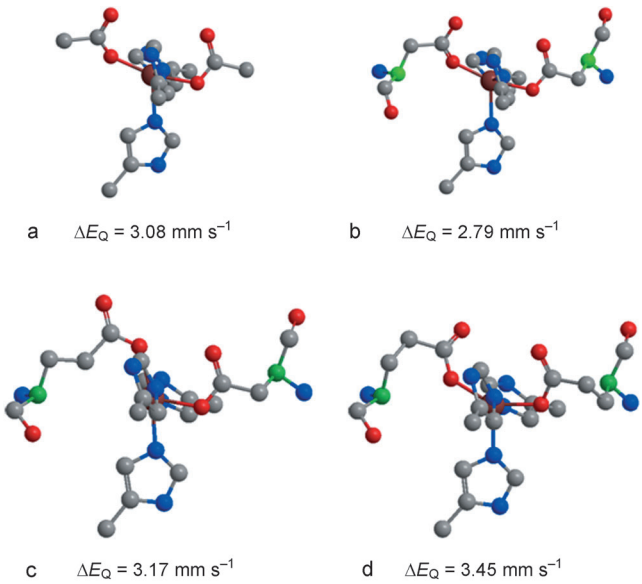

Figure 5. Models of the coordination sphere of Fe^{2+} in PerR and Fur mutants; N blue, O red, Fe brown, C gray, Cα green. The axial His pointing downward is His 93. Left carboxylate (Asp/Glu) is the 104 (108) residue, right carboxylate (Asp/Glu) is the 85 residue. H atoms are not shown. Calculated QS parameters are given (ΔE_Q). a) Starting model structure (see text); b) model structure with Asp85-Asp104; c) model with single Glu104 mutation; d) model with double Glu85-Glu104 mutations.

procedure was used to define and optimize the models, while freezing in space the main structural constraints provided by the protein structure, that is, Cα, NH, and CO atoms from main chain Asp/Glu residues and His group positions. This procedure is justified by the comparison of *Bs* PerR-Zn-Mn and *Hp* Fur-Zn-Zn X-ray crystal structures that reveal only small displacements of the protein chain in this region.[11]

Our approach proved to be quite successful, as we were able to identify optimized structures for the three model sites (Asp85-Asp104, Asp85-Glu104, and Glu85-Glu104), with calculated QS in very good agreement with the experimental trends (Figure 5). In particular, a significant increase in the QS values was associated with each replacement of an aspartate by a glutamate residue. Two other features deserve

attention because they show the consistency of our results. First, the Glu104 binding mode in the Asp85-Glu104 model illustrated in Figure 5c appears similar to that present at the Zn site in *Hp* Fur-Zn-Zn X-ray structure.[11] Second, the Glu85 residue in the Glu85-Glu104 model shown in Figure 5d exhibits a semi-chelating mode of the carboxylate with a reduced Fe–O distance of the second "unbound" oxygen (3.0 Å) in agreement with the "5 + 1" coordination of the iron proposed for *Ec* Fur.[17] Again this model is further supported by the observation that the corresponding glutamate (E90) in the *Hp* Fur-Zn-Zn X-ray crystal structure adopts a chelating binding mode.[11] Moreover the two structures derived from the calculation provide a rationale to explain the insensitivity of the Fur proteins to H_2O_2. Indeed, for the Asp85-Glu104 species model of the *Bs* Fur site the Glu residue has moved upward (Figure 5c) so that it is now trans to His 93. As a consequence, the axis of the square pyramid has rotated approximately 90° from the Fe–N(His93) to the Fe–O-(Asp85) direction, and thus the accessible 6th coordination site on the Fe is now hindered by the Glu104 lateral chain. Finally, in the Glu85-Glu104 model (Figure 5d) the Glu104 is less axial than in the preceding model owing to the fact that Glu85 both moves upward and rotates toward Fe, bringing the second oxygen close to it (3.0 Å). This leads to a constrained situation where the two carboxylates are too close (3.9 Å against 4.8 Å in the initial Asp-Asp site) to each other to allow any interaction of the Fe with H_2O_2.

In summary, our biochemical results clearly established that Asp104 is the key residue that makes PerR sensitive to H_2O_2 whereas Fur with Glu108 is not. Mössbauer spectroscopy studies showed that a change in Fe coordination is associated with the Asp/Glu mutation at this position and another one with further mutation at position 85, although the latter was not important for reactivity. Finally, DFT analyses, validated by calculation of the Mössbauer nuclear parameters, provided a reasonable explanation for the observed reactivity difference in terms of coordination site accessibility. An X-ray crystal structure of a Fur protein with Fe^{2+} or Mn^{2+} in the regulatory site could validate our model. This work further illustrates how the versatility of carboxylate binding modes can be decisive in tuning the reactivity of metalloproteins.

Received: May 10, 2013
Revised: June 24, 2013
Published online: August 12, 2013

Keywords: density functional calculations · ferric uptake regulator · Mössbauer spectroscopy · peroxide stress · peroxide resistance regulator

[1] K. J. Waldron, J. C. Rutherford, D. Ford, N. J. Robinson, *Nature* **2009**, *460*, 823.
[2] Z. Ma, F. E. Jacobsen, D. P. Giedroc, *Chem. Rev.* **2009**, *109*, 4644.
[3] L. Chen, J. D. Helmann, *Mol. Microbiol.* **1995**, *18*, 295.
[4] J. W. Lee, J. D. Helmann, *Nature* **2006**, *440*, 363.
[5] D. A. K. Traoré, A. El Ghazouani, L. Jacquamet, F. Borel, J.-L. Ferrer, D. Lascoux, J.-L. Ravanat, M. Jaquinod, G. Blondin, C. Caux-Thang, V. Duarte, J.-M. Latour, *Nat. Chem. Biol.* **2009**, *5*, 53.
[6] L. Jacquamet, D. A. K. Traoré, J.-L. Ferrer, O. Proux, D. Testemale, J.-L. Hazemann, E. Nazarenko, A. El Ghazouani, C. Caux-Thang, V. Duarte, J.-M. Latour, *Mol. Microbiol.* **2009**, *73*, 20.
[7] J. W. Lee, J. D. Helmann, *J. Biol. Chem.* **2006**, *281*, 23567.
[8] S. A. Mills, M. A. Marletta, *Biochemistry* **2005**, *44*, 13553.
[9] E. Pohl, J. C. Haller, A. Mijovilovich, W. Meyer-Klaucke, E. Garman, M. L. Vasil, *Mol. Microbiol.* **2003**, *47*, 903 – 915.
[10] M. A. Sheikh, G. L. Taylor, *Mol. Microbiol.* **2009**, *72*, 1208.
[11] C. Dian, S. Vitale, G. A. Leonard, C. Bahlawane, C. Fauquant, D. Leduc, C. Muller, H. de Reuse, I. Michaud-Soret, L. Terradot, *Mol. Microbiol.* **2011**, *79*, 1260.
[12] J. Butcher, S. Sarvan, J. S. Brunzelle, J.-F. Couture, A. Stintzi, *Proc. Natl. Acad. Sci. USA* **2012**, *109*, 10047.
[13] A. D. Bochevarov, R. A. Friesner, S. J. Lippard, *J. Chem. Theory Comput.* **2010**, *6*, 3735.
[14] W.-G. Han, G. M. Sandala, D. A. Giammona, D. Bashford, L. Noodleman, *Dalton Trans.* **2011**, *40*, 11164.
[15] M.-E. Pandelia, D. Bykov, R. Izsak, P. Infossi, M.-T. Giudici-Orticoni, E. Bill, F. Neese, W. Lubitz, *Proc. Natl. Acad. Sci. USA* **2013**, *110*, 483 – 488.
[16] J. Katigbak, Y. Zhang, *J. Phys. Chem. Lett.* **2012**, *3*, 3503.
[17] L. Jacquamet, F. Dole, C. Jeandey, J.-L. Oddou, E. Perret, L. Le Pape, D. Aberdam, J.-L. Hazemann, I. Michaud-Soret, J.-M. Latour, *J. Am. Chem. Soc.* **2000**, *122*, 394.

